

Laboratory observation of elastic waves in solids

Thomas D. Rossing and Daniel A. Russell

Department of Physics, Northern Illinois University, DeKalb, Illinois 60115

(Received 21 February 1990; accepted for publication 25 March 1990)

Compressional, torsional, and bending waves in bars and plates can be studied with simple apparatus in the laboratory. Although compressional and torsional waves show little or no dispersion, bending waves propagate at a speed proportional to \sqrt{f} . Reflections at boundaries lead to standing waves that determine the vibrational mode shapes and mode frequencies. Boundary conditions include free edges, simply supported edges, and clamped edges. Typical mode shapes and mode frequencies for rectangular bars, circular plates, and square plates are described.

I. INTRODUCTION

There are many different types of waves in nature. Wave motion has always been a unifying theme throughout physics. The study of waves draws us into nearly all the traditional branches of physics: mechanics, thermodynamics, electromagnetism, quantum mechanics, light, and sound.

One of the authors recently had the pleasure of reviewing a reprinted textbook¹ from the 1960s when unified courses on wave motion were a part of most physics curricula. Unfortunately, many students these days do not experience the benefits of such a course. Furthermore, their laboratory experience with waves is limited, perhaps, to brief encounters with transverse waves on a stretched string, sound waves in an air-filled resonance tube, and visible light waves. Even in high-school physics courses, highly instructive ripple tank experiments are giving way to computer simulations. This trend is an unfortunate one, we believe.

The purpose of this paper is to call attention to some interesting properties of mechanical waves in elastic solids, and to describe three laboratory experiments on wave propagation in bars and plates that can be done with inexpensive equipment in the introductory or intermediate laboratory. They also form the basis for extended experiments using more sophisticated equipment.

As in all wave experiments, the student should be reminded of the similarities in wave behavior. For example, the dispersion relationship for bending waves in a thin bar is quite similar to that of the de Broglie waves associated with a free electron.

II. WAVE PROPAGATION IN SOLIDS

The foundation for wave propagation in solids, as in fluids, lies in three conservation laws: conservation of energy, conservation of momentum, and conservation of mass. These conservation laws can be expressed either in the Lagrangian or Eulerian representation, depending upon whether the boundary conditions are relatively fixed or moving. In a fluid, it is common to use the Eulerian description, in which the velocity, at a certain position and time, refers to the fluid element that happens to be at that position. In a solid, on the other hand, it is usually more convenient to use the Lagrangian description in which the motion of a particular element of the solid is followed.² A compact history of the study of wave propagation in elastic solids is given by Davis.³

2. Longitudinal waves in a bar

The best waves to consider first are the quasi-longitudinal compressional waves in a thin bar or rod, which propa-

gate at a speed given by

$$c_L = \sqrt{E/\rho}, \quad (1)$$

where E is Young's modulus and ρ is density. These waves are called quasi-longitudinal for the following reason: Although the transverse stresses are zero, the transverse strains are not; as a rod stretches, it grows thinner. The ratio between the longitudinal strain ϵ_{11} and the transverse strain ϵ_{22} is Poisson's ratio $\nu = -\epsilon_{22}/\epsilon_{11}$. (Likewise, Young's modulus is defined as the ratio of axial stress to axial strain in a thin rod.)

Compressional waves in a thin bar or rod are described by a one-dimensional wave equation of second order: $\partial^2 w / \partial t^2 = c_L^2 \partial^2 w / \partial x^2$, where $w(x,t)$ is the axial displacement of a small volume element. The general solution of this wave equation is the d'Alembert solution: $w = f_1(c_L t - x) + f_2(c_L t + x)$, where f_1 and f_2 are arbitrary functions and the waves are nondispersive (i.e., their speed c_L does not depend on frequency).

In a thick bar or rod, the longitudinal wave speed decreases slightly at high frequency due to the effects of lateral inertia. According to Love's theory, the longitudinal wave speed is approximately $c'_L = c_L / (1 + \nu^2 K^2 k^2)^{1/2}$, where ν is Poisson's ratio, K is the radius of gyration for the cross section (half the radius for a rod of circular cross section), and k is the wave number.⁴

B. Torsional waves in a bar

A lateral displacement η which varies with x gives rise to a shear strain $\epsilon_{12} = \partial\eta/\partial x$. For small deformations, the shear stress σ_{12} is proportional to the strain, and we define the shear modulus G as the ratio of stress to strain ($G = \sigma_{12}/\epsilon_{12}$) in a thin rod. In a thin rod, torsional shear waves travel at a speed given by

$$c_T = \sqrt{G/\rho}, \quad (2)$$

which is always less than longitudinal wave speed. In fact, G and E are related by the equation $E = 2G(1 + \nu)$, so $c_T/c_L = [2(1 + \nu)]^{-1/2}$. For aluminum, $\nu = 0.33$, and so the ratio of torsional to longitudinal wave speed in a round aluminum rod is 0.61. The wave equation for torsional waves is also a one-dimensional wave equation $\partial^2 \theta / \partial t^2 = c_T^2 \partial^2 \theta / \partial x^2$, so torsional waves are nondispersive.

The torsional wave speed in a bar of rectangular cross section is less than that of a rod with circular cross section. For square cross section, $c_T = 0.92\sqrt{G/\rho}$; when the width is twice the thickness, $c_T = 0.74\sqrt{G/\rho}$; when the width w is more than six times the thickness h , $c_T = 2(h/w)\sqrt{G/\rho}$.

Torsional modes in a bar or rod with free ends have frequencies equal to the torsional wave speed times $n/2L$, analogous to the longitudinal modes. If one end of the bar is clamped, the frequencies and $mc_T/4L$ ($m = 1, 3, 5, \dots$).

C. Bending waves in a bar

Although the compressional and torsional wave speeds in a bar show little or no dispersion (i.e., frequency dependence), this is definitely not the case with bending waves, whose speed is nearly proportional to \sqrt{f} . Bending waves involve both compressional and shear strains.

When a bar is bent, the outer side is stretched and the inner side is compressed; somewhere between is a neutral axis whose length remains unchanged. The simplest theory for such bending motion is the Euler–Bernoulli beam theory, which gives accurate results in thin bars and rods at low frequency. The Euler–Bernoulli equation of motion can be written

$$\frac{\partial^2 y}{\partial t^2} = \frac{-EK^2}{\rho} \frac{\partial^4 y}{\partial x^4}, \quad (3)$$

where E is Young's modulus, K is the radius of gyration for the cross section, and ρ is density. This equation of motion differs from the wave equations for compressional and torsional waves in that it is a *fourth-order* equation; $f(vt \pm x)$ is not a solution. Harmonic solutions may be obtained by substituting $y(x,t) = Y(x)e^{j\omega t}$, giving a solution with four arbitrary constants to be determined from the end conditions,

$$Y(x) = A \cosh(\omega x/v) + B \sinh(\omega x/v) + C \cos(\omega x/v) + D \sin(\omega x/v). \quad (4)$$

Harmonic waves propagate at a phase velocity that is proportional to the square root of frequency and also to the square root of the longitudinal wave speed c_L :

$$v = \sqrt{2\pi f c_L}. \quad (5)$$

The dispersion relationship $\omega = c_L K k^2$ has the same form as that of de Broglie waves for a free particle. The group

velocity is twice the phase velocity ($v_g = d\omega/dk = 2v$).

Although the relatively simple Euler–Bernoulli beam theory gives an accurate description of bending waves in a thin beam or rod at low frequency, it predicts too low a wave speed in a thick bar or a bar vibrating at high frequency. For one thing, it assumes that plane sections remain plane, which is equivalent to neglecting shear deformations. For another thing, it neglects rotary inertia. In Timoshenko beam theory, appropriate terms are added to the equation of motion to account for the effects of shear deformation and rotary inertia.^{5,6}

1. End conditions

The modes of transverse vibration in a bar or rod depend upon the end conditions. Three different end conditions are commonly considered: free, simply supported (hinged), and clamped. For each of these a pair of boundary conditions can be written. At a free end, there is no torque and no shearing force, so the second and third derivatives are both zero; at a simply supported end, there is no displacement and no torque, so y and its second derivative are zero; at a clamped end, y and its first derivative are zero.

$$\text{Free end: } \frac{\partial^2 y}{\partial x^2} = 0, \quad \frac{\partial^3 y}{\partial x^3} = 0; \quad (6a)$$

$$\text{Supported end: } y = 0, \quad \frac{\partial^2 y}{\partial x^2} = 0; \quad (6b)$$

$$\text{Clamped end: } y = 0, \quad \frac{\partial y}{\partial x} = 0. \quad (6c)$$

There are six different combinations of these end conditions, each leading to a different set of vibrational modes. Three of the more common combinations are shown in Fig. 1.

2. Modes of a bar with free ends

Applying the boundary condition (6a) to both ends of a bar leads to an equation⁷

$$\tan(\omega L/2v) = \pm \tanh(\omega L/2v), \quad (7)$$

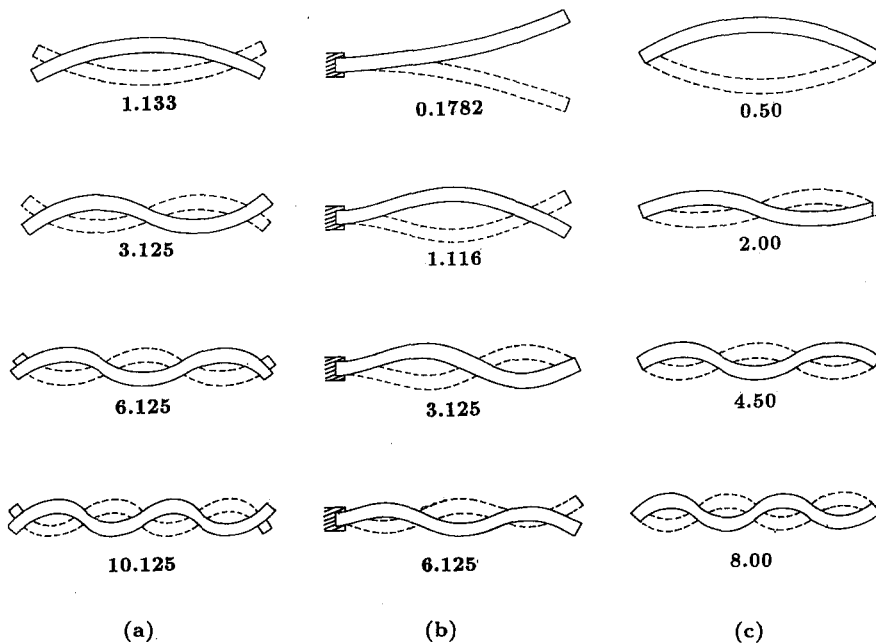


Fig. 1. Bending vibrations of a bar or rod with three different sets of end conditions: (a) both ends free; (b) one clamped end, one free end; (c) two supported (hinged) ends. The numbers are relative frequencies; to obtain actual frequencies, multiply by $\pi K/L^2 \sqrt{E/\rho}$.

Table I. Characteristics of transverse vibrations in a bar with free ends.

Frequency (Hz)	Wavelength (m)	Nodal positions (m from end of 1-m bar)
$f_1 = 3.5607 (K/L^2)\sqrt{E/\rho}$	$1.330L$	0.224, 0.776
$2.756 f_1$	$0.800L$	0.132, 0.500, 0.868
$5.404 f_1$	$0.572L$	0.094, 0.356, 0.644, 0.906
$8.933 f_1$	$0.445L$	0.073, 0.277, 0.500, 0.723, 0.927

where v is the phase velocity in (5). Solution of this transcendental equation gives a set of frequencies

$$f_n = \frac{\pi K}{8L^2} \sqrt{\frac{E}{\rho}} (2n + 1)^2 = \frac{0.113h}{L^2} \sqrt{\frac{E}{\rho}} (2n + 1)^2, \quad n = 1, 2, 3, \dots \quad (8)$$

where h is the thickness of the bar [greater precision results from using (3.011) in place of (3.0) when $n = 1$]. The frequencies and nodal positions for the first four bending modes of a bar with free ends are given in Table I.

D. Waves in a thin plate

Like a bar, a plate can transmit compressional waves, shear waves, torsional waves, or bending waves; and it can have three different boundary conditions: free, clamped, or simply supported (hinged).

A plate might be expected to transmit longitudinal (compressional) waves at the same velocity as a bar: $c_L = \sqrt{E/\rho}$. This is not quite the case, however, since the slight lateral expansion that accompanies a longitudinal compression is constrained in the plane of the plate, thus adding a little additional stiffness. The correct expression for the velocity of longitudinal waves in an infinite plate is

$$c_L = \sqrt{E/\rho(1 - \nu^2)}, \quad (9)$$

where ν is Poisson's ratio ($\nu \approx 0.3$ for most materials).

Actually, pure longitudinal waves occur only in solids whose dimensions in all directions are greater than a wavelength. Such waves travel at a speed c'_L that is slightly less than the quasi-longitudinal waves that propagate in a bar or a plate.

$$c'_L = \sqrt{(E(1 - \nu)/\rho(1 + \nu)(1 - 2\nu))}. \quad (10)$$

Transverse waves in a solid involve mainly shear deformations, although both shear stresses and normal stresses may be involved. Solids not only resist changes in volume (as do fluids), but they resist changes in shape as well. Plane transverse waves occur in bodies that are large compared to the wavelength in all three dimensions, but also in flat plates of uniform thickness.⁸ Transverse waves propagate at the same speed as torsional waves in a circular rod: $c_T = \sqrt{G/\rho}$. The shear modulus G is considerably smaller than Young's modulus E , so transverse and torsional waves propagate at roughly 60% of the speed of longitudinal waves. The radiation of sound in both cases is rather insignificant compared to the case of bending waves that we now discuss.

The equation of motion for bending or flexural waves in a plate is

$$\frac{\partial^2 z}{\partial t^2} + \frac{Eh^2}{12\rho(1 - \nu^2)} \nabla^4 z = 0, \quad (11)$$

where ρ is density, ν is Poisson's ratio, E is Young's modulus, and h is the plate thickness. For harmonic solutions $z = Z(x, y) e^{i\omega t}$:

$$\nabla^4 Z - [12\rho(1 - \nu^2)\omega^2/Eh^2]Z = \nabla^4 Z - k^4 Z = 0, \quad (12)$$

where $k^2 = (\sqrt{12}\omega/h)\sqrt{\rho(1 - \nu^2)/E} = \sqrt{12}\omega/c_L h$. Bending waves in a plate are also dispersive; that is, their velocity v depends upon the frequency

$$v(f) \doteq \omega/k = (\omega hc_L/\sqrt{12})^{1/2} = \sqrt{1.8fhc_L}. \quad (13)$$

The dispersion relation is the same as that of a thin bar or rod: $\omega = c_L K k^2 = c_L h \sqrt{12} k^2$. The values of k that correspond to the normal modes of vibration depend, of course, on the boundary conditions.

E. Circular plates

For a circular plate, ∇ is expressed in polar coordinates, and $Z(r, \phi)$ can be a solution of either $(\nabla^2 + k^2)Z = 0$ or $(\nabla^2 - k^2)Z = 0$. Solutions of the first equation contain the ordinary Bessel functions $J_m(kr)$, solutions to the second the hyperbolic Bessel functions $I_m(kr) = j^{-m} J_m(jkr)$. Thus the possible solutions are given by a linear combination of these Bessel functions times an angular function:

$$Z(r, \phi) = \cos(m\phi + \alpha) [AJ_m(kr) + BI_m(kr)]. \quad (14)$$

In comparing Eqs. (4) and (14), it may be noted that the hyperbolic Bessel functions are to the hyperbolic sines and cosines as the ordinary Bessel functions are to the ordinary sines and cosines.

If the plate is clamped at its edge $r = a$, then $Z = 0$ and $\partial Z/\partial r = 0$. The first of these conditions is satisfied if $AJ_m(ka) + BI_m(ka) = 0$, and the second if $AJ'_m(ka) + BI'_m(ka) = 0$.

A plate with a free edge is more difficult to handle mathematically. The boundary conditions used by Kirchhoff lead to a rather complicated expression for k_{mn} , which reduces to $(2n + m)\pi/2r$ for large ka .⁹ The modal frequencies f_{mn} are given in Table II for modes with m nodal diameters and n nodal circles.

Chladni¹⁰ observed that the addition of one nodal circle raised the frequency of a circular plate by about the same amount as adding two nodal diameters, a relationship that Rayleigh⁹ calls Chladni's law. For large values of ka , $ka \approx (m + 2n)\pi/2$, so that f is proportional to $(m + 2n)^2$. The modal frequencies in a variety of circular plates can be fitted to families of curves: $f_{mn} = c(m + 2n)^p$. In flat plates, $p = 2$, but in nonflat plates (cymbals, bells, etc.), p is generally less than 2.¹¹

Table II. Vibration frequencies of a thin circular plate with free edge.

...	...	$f_{20} = 0.2413 c_L h / a^2$	$f_{30} = 2.328 f_{20}$	$f_{40} = 4.11 f_{20}$	$f_{50} = 6.30 f_{20}$
$f_{01} = 1.73 f_{20}$	$f_{11} = 3.91 f_{20}$	$f_{21} = 6.71 f_{20}$	$f_{31} = 10.07 f_{20}$	$f_{41} = 13.92 f_{20}$	$f_{51} = 18.24 f_{20}$
$f_{02} = 7.34 f_{20}$	$f_{12} = 11.40 f_{20}$	$f_{22} = 15.97 f_{20}$	$f_{32} = 21.19 f_{20}$	$f_{42} = 27.18 f_{20}$	$f_{52} = 33.31 f_{20}$

F. Rectangular plates

Since each edge of a rectangular plate can have any of the three boundary conditions described by Eq. (6) (free, clamped, or simply supported), there are 27 different combinations of boundary conditions, and each leads to a different set of vibrational modes. Our discussion will be limited to three cases in which the same boundary conditions apply to all four edges.

1. Simply supported edges

The equation of motion is easily solved by writing the solutions as a product of three functions of single variables x , y , and t . the displacement amplitude is given by

$$Z(x,y) = A \sin[(m + 1)\pi x/L_x] \sin[(n + 1)\pi y/L_y], \tag{15}$$

where L_x and L_y are the plate dimensions, and m and n are integers (beginning with zero). The corresponding vibration frequencies are

$$f_{mn} = 0.453c_L h \left[\left(\frac{m + 1}{L_x} \right)^2 + \left(\frac{n + 1}{L_y} \right)^2 + \frac{2(m + 1)(n + 1)}{L_x L_y} \right]. \tag{16}$$

The displacement is similar to that of a rectangular membrane, but the modal frequencies are not. Note that the nodal lines predicted by (15) are parallel to the edges; this is not the case for plates with free or clamped edges, as we shall see.

It is convenient to describe a mode in a rectangular plate by (m,n) where m and n are the numbers of nodal lines in the y and x directions, respectively (not counting nodes at the edges). The fundamental mode is designated $(0,0)$.

2. Free edges

Calculating the modes of a rectangular plate with free edges was described by Rayleigh as a problem "of great difficulty." However, Rayleigh's own methods lead to ap-

proximate solutions that are close to measured values, and refinements by Ritz bring them even closer. Results of many subsequent investigations are summarized by Leissa.¹²

The limiting shapes of a rectangle are the square plate and the thin bar. The modes of a thin bar with free ends have the frequencies given by (8). The n th mode has n nodal lines perpendicular to the axis of the bar. As the bar takes on appreciable width, bending along one axis causes bending in a perpendicular direction. This comes about because the upper part of the bar above the neutral axis becomes longer (and thus narrower), while the lower part becomes shorter (and thus wider). Poisson's ratio ν is a measure of the lateral contraction that accompanies a longitudinal expansion in a plate, and the factor $1 - \nu^2$ appears in the expressions for both longitudinal and bending wave velocities [(9) and (13)].

Several bending modes in a rectangular plate can be derived from the bending modes of a bar. The $(m,0)$ modes might be expected to have nodal lines parallel to one pair of sides, and the $(0,n)$ modes would have nodes parallel to the other pair of sides. Due to the coupling between bending motions in the two directions, however, the modes are not pure bar or beam modes. The nodal lines become curved, and the plate takes on a sort of saddle shape (i.e., concave in one direction but convex in the perpendicular direction), which can be called *anticlastic* bending.

It is interesting to note how the combinations develop in a rectangle as L_x/L_y approaches unity. Figure 2 shows the shapes of two modes that are descendants of the $(2,0)$ and $(0,2)$ bar modes in rectangles of varying L_x/L_y . When $L_x = 4L_y$, the $(2,0)$ and $(0,2)$ modes appear quite independent. However, as $L_y \rightarrow L_x$, the beam modes mix together to form two new modes. In the square, the mixing is complete, and two combinations are possible depending upon whether the component modes are in phase or out of phase.

The first ten modes of a square plate with free edges are shown in Fig. 3. The mode of lowest frequency, the $(1,1)$ mode, is a torsional mode in which opposite corners move

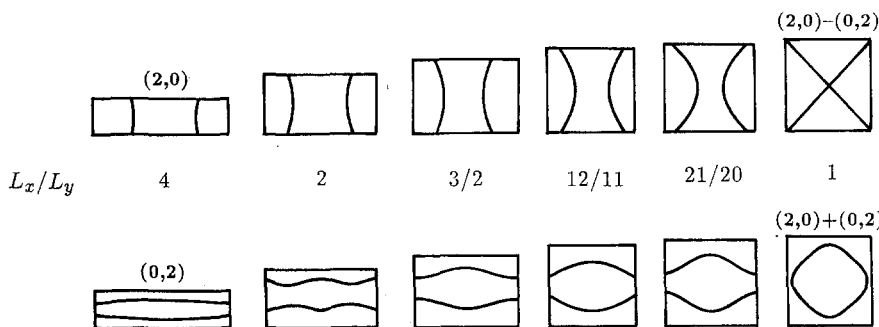


Fig. 2. Mixing of the $(2,0)$ and $(0,2)$ modes in rectangular plates with different L_x/L_y ratios (after Ref. 18).

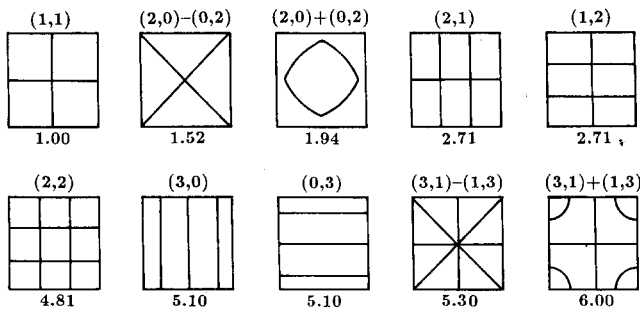


Fig. 3. The first ten modes of an isotropic square plate with free edges. The modes are designated by m and n , the numbers of nodal lines in the two directions, and the relative frequencies for a plate with $\nu = 0.3$ are given below the figure.

in phase. Its frequency is given by

$$f_{11} = \frac{c_T}{2L} = \frac{h}{L^2} \sqrt{\frac{E}{2\rho(1+\nu)}} = \frac{hc_L}{L^2} \sqrt{\frac{1-\nu}{2}} \quad (17)$$

Note that the $(2,0 + 0,2)$ mode ("ring mode") has a higher frequency than the $(2,0 - 0,2)$ mode ("X mode"). In

the X mode, the bending motions characteristic of the $(2,0)$ and $(0,2)$ beam modes aid each other through an elastic interaction that we call Poisson coupling, since its strength depends upon the value of Poisson's ratio.¹³ In the $(2,0 + 0,2)$ ring mode, however, there is an added stiffness due to the fact that the $(2,0)$ and $(0,2)$ bending motions oppose each other. Thus the Poisson coupling splits a modal degeneracy that otherwise would have existed in a square plate. The ratio of the $(2,0 + 0,2)$ and $(2,0 - 0,2)$ mode frequencies is¹⁴

$$f_+/f_- = \sqrt{(1 + 0.7205\nu)/(1 - 0.7205\nu)} \quad (18)$$

Note that the $(2,1)$ and $(1,2)$ modes form a degenerate pair, as do the $(3,0)$ and $(0,3)$ modes. However, Poisson coupling removes the degeneracy in the case of the $(3,1) \pm (1,3)$ pair just as it does in the $(2,0) \pm (0,2)$ case. The general rule is that a nondegenerate pair of modes $(m,n \pm n,m)$ exists in a square plate when $m - n = \pm 2, 4, 6, \dots$

The modal frequencies in an aluminum plate with varying length-to-width ratio are shown in Fig. 4. In this case L_x was kept constant as L_y was varied, so the frequency of the $(3,0)$ mode, for example, is unchanged. The $(1,1)$ mode has a slope of 1. The $(0,3)$ bending mode has a slope

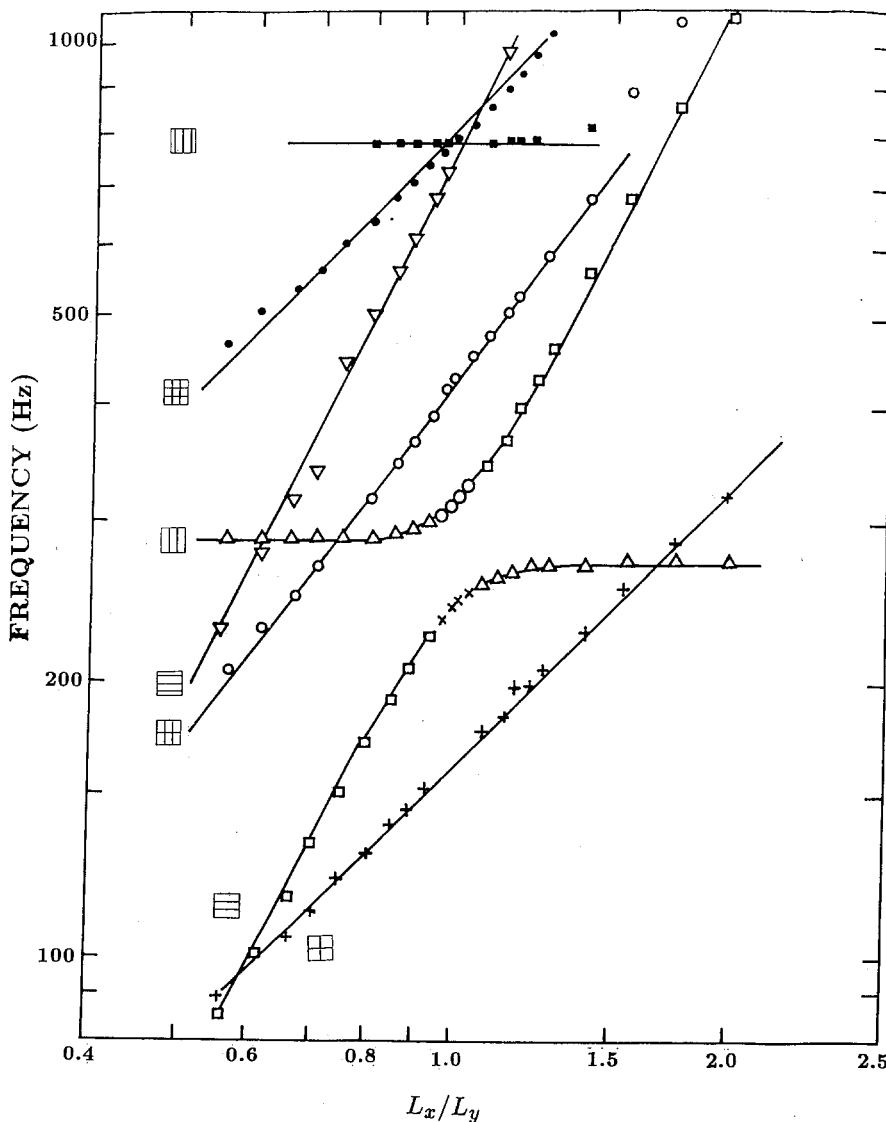


Fig. 4. Modal frequencies of an aluminum plate with varying length-to-width ratio L_x/L_y (Ref. 13).

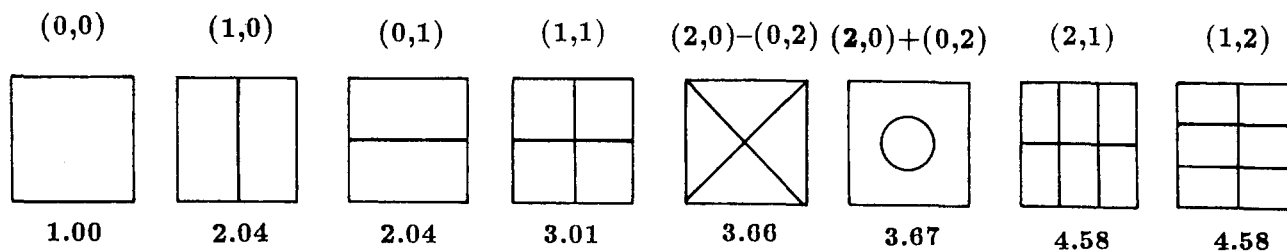


Fig. 5. Nodal patterns for the first eight modes of a square plate with clamped edges. Relative frequencies are given below the patterns.

of 2, as does the (0,2) mode above and below the region of $L_x = L_y$. The (2,1) mode, which combines twisting and bending motions, has a slope of about $\frac{4}{3}$.

3. Clamped edges

The first eight modes of a square plate with clamped edges are shown in Fig. 5. There is considerable variation in the mode designation by various authors, and so we have used the same designation that was used in Sec. II F 1 for a plate with simply supported edges: m and n are the numbers of nodes in the directions of the y and x axes, respectively, not counting the nodes at the edges. The fundamental (0,0) mode has a frequency: $f_{00} = 1.654 c_L h / L^2$, where h is the thickness, L is the length, and $c_L = \sqrt{E\rho^{-1}(1-\nu^2)^{-1}}$ is the longitudinal wave velocity.¹² The relative frequencies of the modes are given below the patterns in Fig. 5.

Comparing the modes of the square plate with clamped edges to one with free edges, we note that

(1) The (1,1) mode has a frequency nearly 10 times greater than (1,1) mode in a free plate.

(2) Three other modes exist below the (1,1) mode in the clamped plate.

(3) The X mode and ring mode are only about 0.5% different in frequency, and the diameter of the ring mode is smaller than it is in a free plate.

(4) Nondegenerate mode pairs ($m, n \pm n, m$) exist when $m - n = \pm 2, 4, 6, \dots$, as in the free plates, but the transition from modes characteristic of rectangular plates to those of square plates changes much more abruptly as $L_x \rightarrow L_y$ in clamped plates than in free plates.¹⁴

Relative frequencies of rectangular plates with clamped edges are given in Table III. The actual frequencies can be obtained by multiplying the relative frequencies by $1.654 c_L h / L_y^2$.

III. EXPERIMENT 1: WAVES IN A BAR

We want to observe three types of standing waves in an aluminum bar: (1) longitudinal compressional waves; (2)

transverse bending waves; (3) torsional waves. Bending waves are dispersive, whereas compressional and torsional waves are not. In all three cases, we employ a bar of rectangular cross section with free ends.

To excite a single mode of vibration or standing wave pattern in a bar we can apply a sinusoidal driving force at the appropriate frequency or we can apply an impact while the bar is restrained at the nodal positions for the desired mode. For demonstrating modes of vibration in a lecture, impact excitation (e.g., striking the bar with a hammer or even banging the end on the floor) is most dramatic; for identifying a large number of modes, however, sinusoidal excitation is preferred. More sophisticated methods for modal analysis, such as holographic interferometry and the use of force hammers and accelerometers, will not be discussed in this paper. Rather, we describe a very simple but versatile experimental arrangement.

A. Experimental method

The simple arrangement recommended for this experiment is shown in Fig. 6. The bar is supported by two rubber bands, and a small cylindrical magnet is attached. A coil of about 300–400 turns, driven by an audio amplifier, supplies an alternating magnetic field. In order to determine the modal shapes (i.e., the motion of the bar as a function of position), a small electret microphone (e.g., Radio Shack 33-1052 tie clip microphone, about \$12) is used to scan the sound field near the bar.¹⁵

Although the output of the microphone (a few millivolts for one of the stronger modes) can go directly to an oscilloscope, we find it convenient to amplify and filter it using an octave-band filter set (equalizer) of the type sold in audio equipment stores (from \$50 and up). This is especially useful if the experiment is to be done in a noisy room. If the equalizer has no microphone input, we add a simple preamplifier with input and output jacks; if the equalizer has a microphone input, only a preamplifier output jack is necessary. Connecting the two channels of a typical stereo equalizer in series provides a nominal 24-dB gain at the octave-band center frequency.¹⁶ Although octave-band filters greatly improve the signal-to-noise ratio at the frequency of interest, they introduce considerable phase distortion, which can be reduced by increasing the gain of the filters just above and below the principal octave-band filter (thus increasing the bandwidth). Because of the phase distortion problem, we switch out the filters when they are not needed in the laboratory.

Nodal lines are most easily located by observing abrupt changes in the phase of the sound field (by means of a Lissajous pattern on the oscilloscope) as the microphone is moved along the bar. In order to maintain a nearly constant spacing as the microphone is moved, it is convenient to clip

Table III. Relative vibrational frequencies of rectangular plates with clamped edges.¹²

Mode	$L_x/L_y = 1$	1.5	2	2.5	3	∞
(0,0)	1.00	0.75	0.68	0.66	0.64	0.62
(0,1)	2.04	1.88	1.82	1.79	1.78	1.72
(1,0)	2.04	1.16	0.88
(1,1)	3.01	2.27	2.02	1.91	1.86	1.72

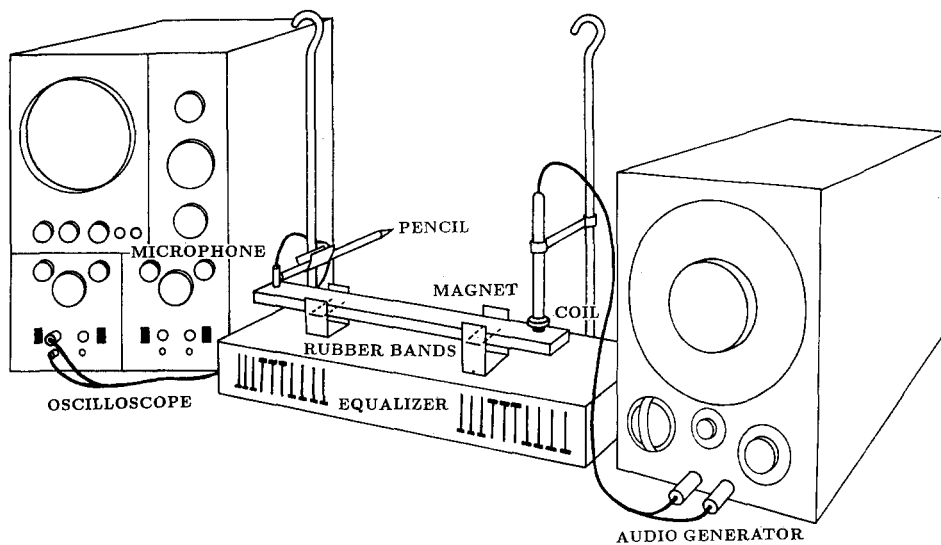


Fig. 6. Arrangement used for observing standing waves in an aluminum bar.

the tie clasp holder (if the tie clip microphone is used) to a pencil supported by a ring stand or a weight hanger (as shown in Fig. 6).

To excite longitudinal waves, the driver magnet is attached to the end of the bar. Transverse bending waves and torsional waves can be excited by attaching the magnet near one corner of the largest face of the bar. Waves characterized by bending in the plane of the bar require that the magnet be attached to an edge of the bar. Although inexpensive ceramic magnets (\$11 per hundred, Edmund Scientific) are adequate for exciting most modes of vibration, neodymium-iron-boron "super" magnets (\$2.55 each, General Science Materials) are advantageous for the higher frequencies. We employ driving coils matched to the 50- Ω output of an audio generator or to the lower impedance of an audio amplifier (the 16- Ω output, if the amplifier has one). (In designing the drive coils, one shouldn't forget the inductive reactance of the coil as well as its resistance). A typical magnet-coil driver of this type should provide a force amplitude of 0.1–0.5 N up to 5000 Hz.

B. Experimental results

Modal frequencies for 39 modes of an aluminum bar with dimensions $35.6 \times 3.8 \times 0.95$ cm, covering the frequency range 440–37 800 Hz, are shown in Fig. 7 and in Table IV. Fitted to the data in Fig. 7 are straight lines having slopes ($\log f_n / \log n$) of 1 (longitudinal and torsional modes) or 2 (bending modes). Obviously, the modes of high frequency are quite difficult to identify. In a 2-hour laboratory, however, it is quite reasonable to map the modal shapes of 5 to 7 bending and torsional modes up to 5700 Hz plus a couple of longitudinal modes at higher frequency.

In the bar in Fig. 7, the first torsional mode has a frequency close to that of the third bending mode (1956 vs 2115 Hz). The resonances are sharp, however, so there is little difficulty in identifying the two separate modes. (Torsional modes have a longitudinal nodal line at the center of the bar.) At a frequency midway between two modal frequencies, it is sometimes possible to observe motion which combines these two normal modes.

Table IV includes the modal frequencies and also the corresponding wave speeds calculated from these frequen-

cies. The bending wave speeds are nearly proportional to \sqrt{f} , as predicted by thin bar theory, although speeds for the higher modes fall slightly below this prediction, in keeping with thick bar theory which includes the effects of shear and rotary inertia. The longitudinal wave speed is nearly constant, but at the higher frequencies it decreases slightly below the value $\sqrt{E/\rho}$ due to lateral inertia. The torsional wave velocity, on the other hand, increases slightly with frequency for reasons that are not well understood by the authors.

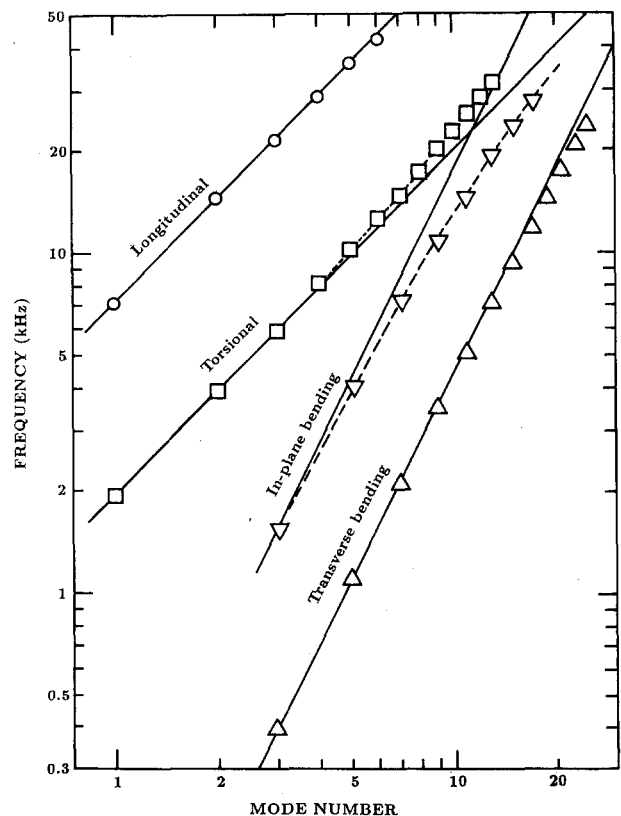


Fig. 7. Modal frequencies for an aluminum bar with dimensions $35.6 \times 3.8 \times 0.95$ cm as a function of mode number n or $2n + 1$.

Table IV. Mode frequencies and corresponding wave velocities in an aluminum bar $35.6 \times 3.8 \times 0.95$ cm.

n	Transverse bending		In-plane bending		Torsional		Longitudinal	
	f_n (Hz)	v (m/s)	f_n (Hz)	v (m/s)	f_n (Hz)	c_T (m/s)	f_n (Hz)	c_L (m/s)
1	384	187	1526	736	1956	1393	7230	5147
2	1084	310	3941	1085	3932	1399	14 434	5139
3	2115	433	7162	1463	5958	1414	21 582	5122
4	3471	555	10 885	1804	8060	1435	28 627	5096
5	5148	676	14 842	2106	10 230	1457	35 500	5055
6	7114	795	19 055	2387	12 507	1484	42 077	4993
7	9345	911	23 278	2638	14 883	1514		
8	11 851	1026	27 565	2871	17 402	1549		
9	14 578	1137			20 050	1586		
10	17 527	1247			22 810	1624		
11	20 600	1352			25 695	1663		
12	23 963	1447			28 677	1702		
13					31 816	1743		

Figure 8 similarly shows the modal frequencies of a rosewood xylophone bar (tuned to F_4^\sharp). Xylophone bars have an arch cut into the lower side to reduce the frequency of the first bending mode more than that of the second one, in order to bring them into the harmonic ratio 1:3. Undercutting the bar in this manner lowers the torsional mode frequencies considerably, but has little effect on the longitudinal modes. (Marimba bars and vibraphone bars have

even deeper arches, so that the first and second bending modes have frequencies in the ratio 1:4.)¹⁷

IV. EXPERIMENT 2. STANDING WAVES IN A CIRCULAR PLATE

A. Experimental method

The apparatus for exciting bending modes in a thin circular aluminum plate is similar to that previously described for a bar. The plate is suspended by three rubber bands or elastic cords. The strong modes at the lower frequencies can (and should) be observed by sprinkling salt or fine powder on the surface to create Chladni patterns,^{10,11,18} but the higher modes are observed better with the microphone scan technique described in Sec. III A.

B. Results

Frequencies of 31 bending modes in an aluminum plate 31 cm in diameter and 0.163 cm thick are shown as a function of the number m of nodal diameters in Fig. 9. The family of modes without nodal circles ($n = 0$) lies along a straight line having a slope $p_0 = 1.93$. In Fig. 9(b), the same data are plotted as a function of $m + 3n$ (modified Chladni's law). Now all the modes can be fitted reasonably well to a line having a slope $p = 2$.

In an earlier paper,¹¹ we showed that the mode frequencies of flat circular plates can be fitted to two modified forms of Chladni's law: $f_{mn} = c(m + 3n)^p$ or $f_{mn} = c_n(m + 2n)^{p_n}$. In the first case, the $2n$ in Chladni's law has been replaced by $3n$; in the second case, constants c_n and p_n are selected for a best fit with data for each value of n . Subsequent experiments have shown that modal frequencies in a wide variety of plates, bells, gongs, and cymbals can be fitted to such modified forms of Chladni's law reasonably well.¹⁹⁻²¹

V. EXPERIMENT 3. STANDING WAVES IN SQUARE PLATES

A. Experimental method

For this experiment, we use two aluminum plates, 30.5 cm (12 in.) square and 1.59 mm ($\frac{1}{16}$ in.) thick. One plate,

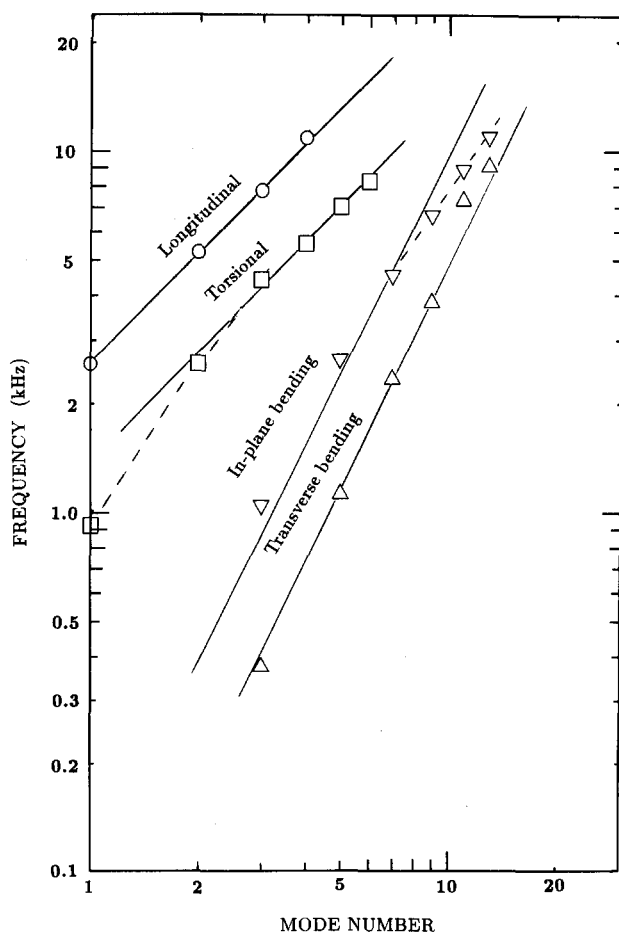


Fig. 8. Modal frequencies of a xylophone bar turned to F_4^\sharp (370 Hz).

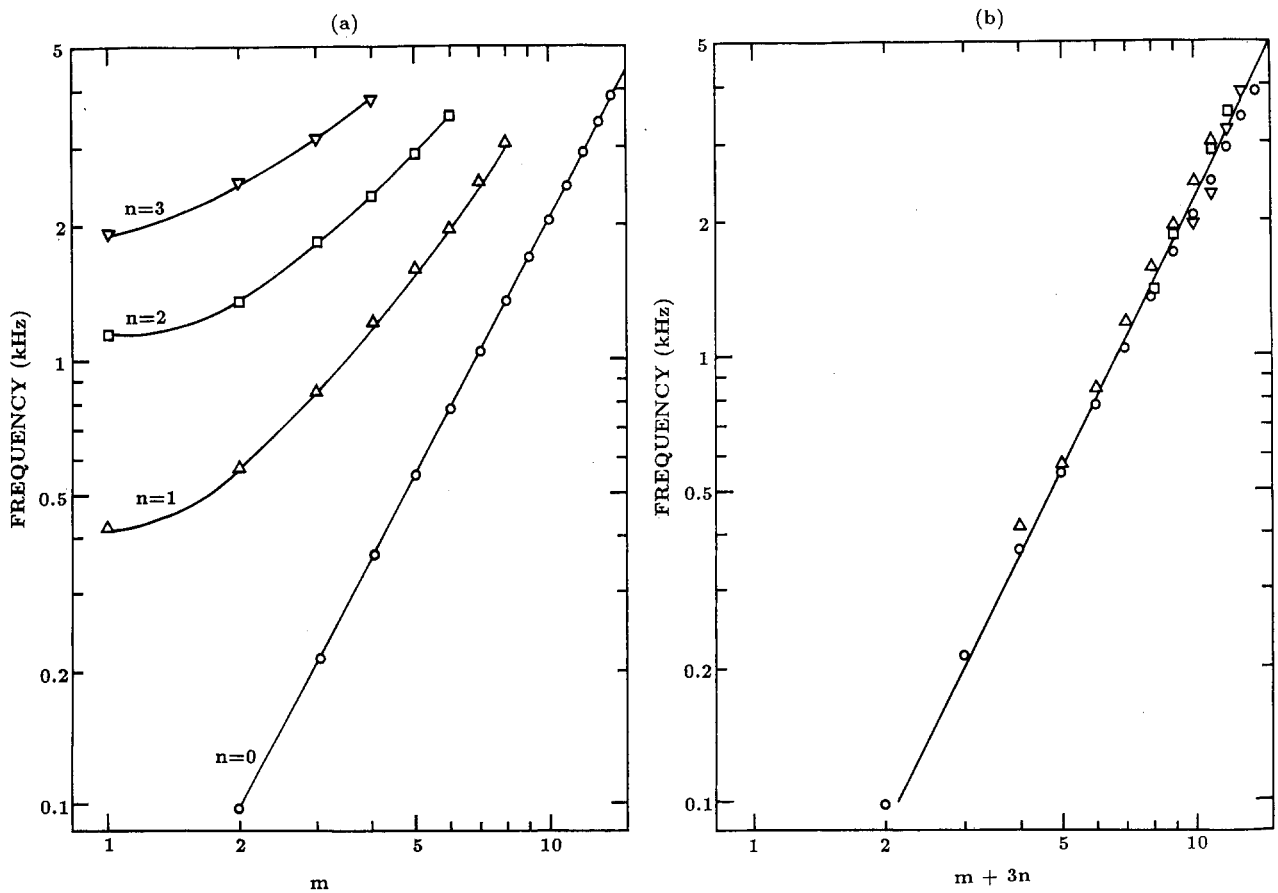


Fig. 9. Modal frequencies f_{mn} of an aluminum plate 31 cm in diameter and 0.163 cm thick. (a) As a function of m with n as a parameter; (b) as a function of $m + 3n$ (modified Chladni's law) with $p = 2$ line shown.

with free edges, is suspended by rubber bands, as in Sec. IV A. The other plate, slightly larger, is clamped in an aluminum frame so that the free portion is the same size as the free plate. In other respects, the experimental method was the same as that used for the circular plate.

B. Results

Modal shapes and frequencies for six modes observed in each plate are shown in Fig. 10. The modal shapes and frequency ratios compare reasonably well with those in

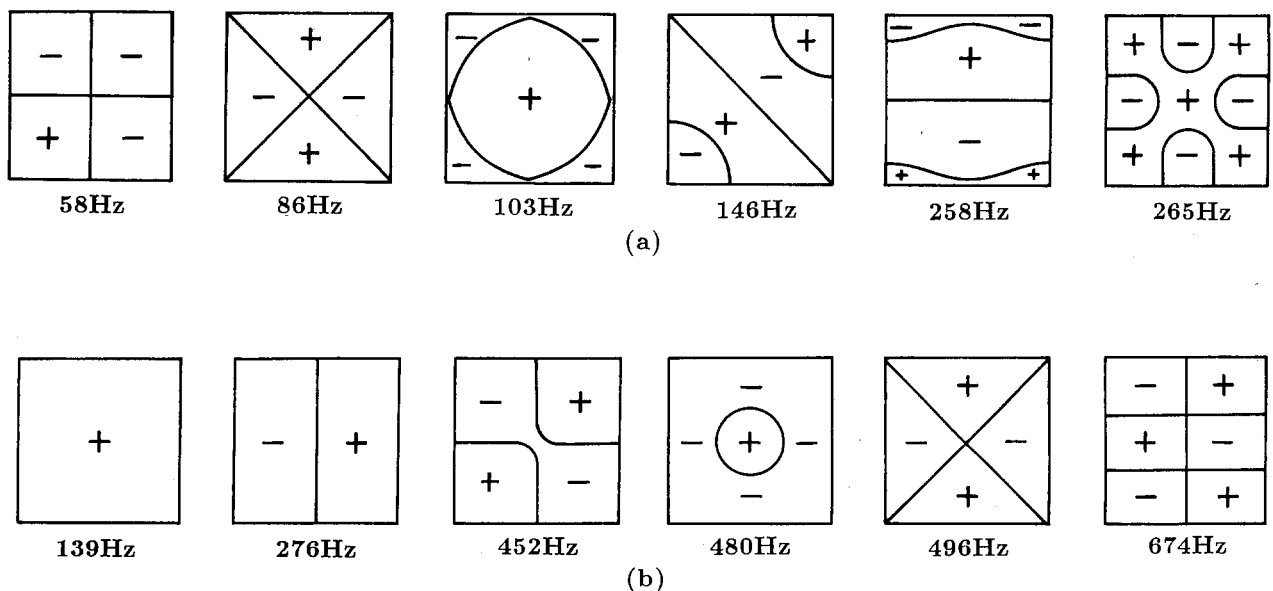


Fig. 10. Mode shape and modal frequencies in a square aluminum plate: (a) free edges; (b) clamped edges.

Fig. 3 (free edges) and Fig. 5 (clamped edges). The fourth mode in the free plate (at 146 Hz) is a combination of the degenerate (3,0) and (0,3) modes in Fig. 10, but the amplitude of the (0,3) mode appears to be much greater than that of the (3,0) mode. (The amplitude ratio depends upon where the force is applied.) The frequency ratio of the ring mode and X mode in Fig. 3(a) (1.20) is slightly less than that calculated from Eq. (18) (1.27 for $\nu = 0.33$).

The modal shapes and frequencies for the clamped plate in Fig. 10(b) are in reasonably good agreement with those in Fig. 6, although all the frequencies are less than the theoretical values, probably because the clamping frame has insufficient mass to clamp the edges firmly. The ring node in the fourth mode has a smaller diameter than in the corresponding free-plate mode in Fig. 10(a).

VI. RECTANGULAR PLATES

Experiments using rectangular plates of aluminum and spruce are described in Ref. 13. In a quarter-cut spruce plate, Young's modulus is about 16 times greater along the grain than across the grain. Thus bending waves travel four times as fast along the grain, and the degeneracy that leads to the appearance of the X mode and ring mode occurs for $L_x = 2L_y$. (In a skew-cut plate, the anisotropy is even greater, and the degeneracy occurs at about $L_x = 3L_y$).¹³ Spruce is widely used as a soundboard material in musical instruments such as pianos, guitars, and violins.

VII. CONCLUSION

Different types of waves can propagate in solids. Some types are dispersive, some are not. Studying standing waves in bars and plates with simple equipment in the laboratory can contribute substantially to understanding wave behavior of all kinds, a unifying theme throughout physics.

¹W. C. Elmore and M. A. Heald, *Physics of Waves* (Dover, New York, 1985) [see review in *Am. J. Phys.* **55**, 670–671 (1987)]. Another excellent textbook on waves from this same period [D. H. Towne, *Wave*

Phenomena (Addison-Wesley, Reading, MA, 1967)] has recently been reprinted by Dover, as well.

²K. V. Ingard, *Fundamentals of Waves and Oscillations* (Cambridge U. P., Cambridge, 1988), Chap. 20.

³J. L. Davis, *Wave Propagation in Solids and Fluids* (Springer-Verlag, New York, 1988), Chap. 8.

⁴K. F. Graaf, *Wave Motion in Elastic Solids* (Oxford U. P., London, 1974), Chap. 2.

⁵See, for example, Eq. (3.4.20) in Ref. 4 or Eq. (7-40) in F. S. Tse, I. E. Morse, and R. T. Hinkle, *Mechanical Vibrations: Theory and Applications* (Allyn and Bacon, Boston, 1963), 2nd ed.

⁶A. E. H. Love, *A Treatise on the Mathematical Theory of Elasticity* (Dover, New York, 1944), 4th ed.

⁷L. E. Kinsler, A. R. Frey, A. B. Coppens, and J. V. Sanders, *Fundamentals of Acoustics* (Wiley, New York, 1982), 3rd ed., p. 75.

⁸L. Cremer, M. Heckl, and E. E. Ungar, *Structure-Borne Sound* (Springer-Verlag, New York, 1973), Chap. 2.

⁹Lord Rayleigh (J. W. Strutt), *The Theory of Sound* (MacMillan, London, 1894; reprinted by Dover, New York, 1945), Vol. 1, 2nd ed., Sec. 219.

¹⁰L. F. F. Chladni, *Die Akustik* (Breitkopf and Härtel, Leipzig, 1830), 2nd ed.

¹¹T. D. Rossing, "Chladni's laws for vibrating plates," *Am. J. Phys.* **50**, 271–274 (1982).

¹²A. W. Leissa, *Vibration of Plates*, NASA SP-160 (NASA, Washington, DC, 1969).

¹³G. Caldersmith and T. D. Rossing, "Determination of modal coupling in vibrating rectangular plates," *Appl. Acoust.* **17**, 33–44 (1984).

¹⁴G. B. Warburton, "The vibration of rectangular plates," *Proc. Inst. Mech. Eng. A* **168**, 371–384 (1954).

¹⁵A simple arrangement of this type was a prizewinner in the AAPT apparatus competition, 1986.

¹⁶T. D. Rossing, "Inexpensive octave-band filters for laboratory and demonstration experiments in acoustics," *Am. J. Phys.* **50**, 1050 (1982).

¹⁷T. D. Rossing, *Science of Sound* (Addison-Wesley, Reading, MA, 1990), 2nd ed., Chap. 13.

¹⁸M. D. Waller, *Chladni Figures: A Study in Symmetry* (Bell, London, 1961).

¹⁹T. D. Rossing and R. B. Shepherd, "Acoustics of cymbals," *Proc. 11th Int. Congr. Acoust. (Paris)* **4**, 329–333 (1983).

²⁰R. Perrin, T. Charnley, H. Banu, and T. D. Rossing, "Chladni's law and the modern English church bell," *J. Sound Vib.* **102**, 11–19 (1985).

²¹T. D. Rossing and R. Perrin, "Vibrations of bells," *Appl. Acoust.* **20**, 41–70 (1987).

THE MUSICAL VERSION OF THE LAWS OF THERMODYNAMICS

- (1) Heat is work, and work is heat.
- (2) Heat won't flow from the colder to the hotter; you can try it if you like, but you'd far better notter.

Michael Flanders and Donald Swann, "The First and Second Laws of Thermodynamics," from *At the Drop of Another Hat*, Angel Records.